International Journal of Solids and Structures 75–76 (2015) 299–308

Contents lists available at ScienceDirect

International Journal of Solids and Structures

journal homepage: www.elsevier.com/locate/ijsolstr

Wave propagation across the imperfectly bonded interface between cracked elastic solid and porous solid saturated with two immiscible viscous fluids

Sushant Shekhar *, Imtiyaz A. Parvez

Academy of Scientific and Innovative Research, New Delhi 110 001, India
CSIR-Fourth Paradigm Institute, Bangalore 560037, India

ARTICLE INFO

Article history:
Received 10 January 2015
Received in revised form 8 July 2015
Available online 5 September 2015

Keywords:
Reflection and refraction
Energy partition
Seismic attenuation
Cracked elastic solid
Saturated porous solid

ABSTRACT

The present study is aimed at understanding the effect of a vertically aligned crack, present in the elastic half space on the propagation of attenuated waves. These waves are incident at a point on the interface between the porous half space and the cracked elastic half space. The analysis is based on Snell's law for reflection and refraction of an incident wave at the interface. A loose bonding at the interface between the porous half space and the cracked elastic half space has been considered and represented here as the tangential slip. The proposed model is solved for the propagation of harmonic plane waves. The final equations are in the form of Christoffel equations from which we find four reflected waves (three longitudinal body waves and one transverse body wave) and two refracted waves (one longitudinal body wave and one transverse body wave). The expression of reflection–refraction coefficients and energy share of each reflected and refracted waves for a given incident wave is obtained in closed form and computed numerically in the present study. Numerical examples are considered for the partition of the incident energy in which we have studied the effect of aspect ratio, crack density and loose bonding parameter.

1. Introduction

Poroelasticity theory is an important theory for the study of the mechanical behavior of porous solids in different fields, some of which are soil dynamics, oil exploration, earthquake engineering, geomechanics and reservoir engineering. The study of wave propagation in a porous solid saturated with a single fluid was started by Biot who has published some important research work related to wave propagation in porous media, Biot (1956a,b, 1962a,b) and Biot and Willis (1957). From his studies Biot has found two longitudinal body waves and one transverse body wave.

Biot's theory has been extended as mixture theory in which the porous medium is saturated by more than one fluid. Brutsaert (1964) first found the presence of a third longitudinal body wave in an unsaturated granular medium. Based on this study, Bedford and Drumheller (1983) have developed theories of immiscible and structured mixtures. Garg and Nayfeh (1986) have discussed the third compressional wave in their study. For low frequency elastic waves, Tuncay and Corapcioglu (1997) have successfully studied the presence of three longitudinal body waves and one transverse body wave in a porous solid saturated with two immiscible fluids for which they had used a volume averaging technique. They found that the first two longitudinal body waves are the same as Biot (1956b) while the third longitudinal body wave is due to the presence of the third fluid. Using this theory, many developments have been carried out by researchers; e.g. Yew and Jogi (1976), Tomar and Arora (2006) and Sharma and Saini (2012).

Deresiewicz (1962) has studied the effect of the boundaries of the liquid filled porous solid on the propagation of a wave that changes the wave pattern of the elastic wave. Deresiewicz and Skalak (1963) have successfully applied Neumann's uniqueness theorem of elasticity to a porous medium for defining the boundary conditions. Based on the previous study, Sharma (2009) has given different cases for the boundary conditions for the porous solid. A study of the reflection and transmission from the interface between two media have been carried out by some researchers e.g. Ainslie and Burns (1995), Borcherdt (1982), Berryman (2007), Denneman et al. (2002), Sharma and Gogna (1991), Sharma (2008a) and Vashisth et al. (1991).

The earth's crust normally has a lot of aligned cracks or micro-cracks which contain fluids or sometimes voids. O'Connell and Budiansky (1974) calculated the effect of cracks on the elastic

* Corresponding author at: CSIR-Fourth Paradigm Institute, Bangalore 560037, India. Tel.: +91 8025051346; fax: +91 8025220392.
E-mail address: sushantshekhar85@yahoo.com (S. Shekhar).

http://dx.doi.org/10.1016/j.ijsolstr.2015.08.022
0020-7683/

properties of an isotropic solid. Most of the cracks are developed due to small earthquakes that have been described in Crampin (1978, 1985, 1987) who found some important aspects related to wave propagation through these cracks. These small earthquakes may result due to the accumulation of stresses in the particular region. The study of cracks inside the earth's crust can give important information related to the oils/water/minerals deposited in these cracks. Fluid flow from a porous medium to the cracked elastic medium can be controlled by some boundary conditions at the interface, those may be fully opened or closed or partially open-closed, as given in Sharma and Gogna (1991), Sharma (1999, 2008a, 2009) and Vashisth et al. (1991). The presence of the attenuation plays an important role in wave propagation through aligned cracks and this phenomena has been shown in Chatterjee et al. (1980) and Xu and King (1990). Currently, Nandan and Saini (2012) have studied the effect of an aligned crack on the reflection and transmission of elastic waves through the interface between the poroelastic solid with one fluid and cracked elastic solid.

For the study of wave propagation, we summarize the previous work in Table 1 based on appropriate criteria. In the present study, we consider an isotropic homogeneous poroelastic medium saturated with a mixture of two immiscible fluids lying over the cracked elastic half space. We assume that the two media are loosely connected to each other and the connected coefficient or bonding parameter is represented here by ψ. The interface between these two media is assumed at $x_3 = 0$. We solve the dynamical equation with the help of the assumed harmonic solution. The obtained results are in the form of Christoffel equations and these results provide four inhomogeneous waves in a porous medium, of which three are longitudinal body waves and one is a transverse body wave. The reflection coefficients and energy share have been solved for given boundary conditions at a loosely bonded interface. The energy matrix defines the distribution of the incident energy to the four reflected waves, two refracted waves and some energy is spent at the interface and is defined as dissipation energy. The final results related to energy share satisfy the conservation law of energy. We graphically demonstrate the results of energy share with respect to the incident angle θ for the effect of aspect ratio c/a (where c is the crack thickness and a is the radius of circular crack), crack density η and bonding parameter ψ. We have also conducted a comparative study between the presence and absence of vertical aligned cracks with respect to the crack density and the crack thickness in the elastic half space. For the numerical validation of the present study, we assume that the first medium is water and CO_2 saturated sandstone and second medium is basaltic rock.

Table 1
Classification of related references by type of systems and chronological order.

Solid	**Porous media**
• Biot and Willis (1957)	• Biot (1956a,b, 1962b,a)
• Achenbach (1973)	• Vashisth et al. (1991)
• O'Connell and Budiansky (1974)	• Tuncay and Corapcioglu (1997)
• Crampin (1978, 1985, 1987)	• Denneman et al. (2002)
• Xu and King (1990)	• Tomar and Arora (2006)
• Ainslie and Burns (1995)	• Nandan and Saini (2012)
• Sharma (1999)	• Sharma and Saini (2012)
Ideal fluids	**Viscous fluids**
• Sharma (2008a)	• Chatterjee et al. (1980)
• Nandan and Saini (2012)	• Tomar and Arora (2006)
	• Sharma and Saini (2012)
Perfect interface	**Imperfect interface**
• Ainslie and Burns (1995)	• Vashisth et al. (1991)
• Denneman et al. (2002)	• Nandan and Saini (2012)
• Tomar and Arora (2006)	
• Sharma and Saini (2012)	
Isotropic	**Anisotropic**
• Tuncay and Corapcioglu (1997)	• Biot and Willis (1957)
• Tomar and Arora (2006)	• Sharma and Gogna (1991)
• Nandan and Saini (2012)	• Vashisth et al. (1991)
• Sharma and Saini (2012)	• Sharma (2008b)

2. Basic theoretical framework

2.1. Poroelastic solid with two immiscible fluids

The balance equation in the absence of body forces for the low frequency vibration in a tri phase solid–air–water mixture can be expressed as Tuncay and Corapcioglu (1997),

$$\langle \tau_s \rangle_{ij,j} = \langle \rho_s \rangle \frac{\partial^2 u_i}{\partial t^2} - d_g \frac{\partial}{\partial t}(v_i - u_i) - d_l \frac{\partial}{\partial t}(w_i - u_i)$$
$$\langle \tau_g \rangle_{ij,j} = \langle \rho_g \rangle \frac{\partial^2 v_i}{\partial t^2} + d_g \frac{\partial}{\partial t}(v_i - u_i)$$
$$\langle \tau_l \rangle_{ij,j} = \langle \rho_l \rangle \frac{\partial^2 w_i}{\partial t^2} + d_l \frac{\partial}{\partial t}(w_i - u_i) \tag{1}$$

where the subscripts s, g, l define solid, gas and liquid phases, respectively. For phase $k(= s, g, l)$, $\langle \tau_k \rangle$'s and $\langle \rho_k \rangle$'s signify the average stresses and average partial density over the solid–gas–liquid aggregate. u_i, v_i and w_i represent the displacement components of solid, gas and liquid particles. Here, the coefficients d_g and d_l define the presence of dissipation related to gas and liquid particles in the porous medium (according to Darcy's law) and these coefficients can be defined here as:

$$d_k = \frac{\mu_k \alpha_k^2}{\vartheta \vartheta_k}, \quad (k = g, l) \tag{2}$$

where the symbol's μ_k, ϑ_k, and α_k represent the viscosity, relative permeability and volume fractions for each fluid and ϑ represents the intrinsic permeability of the porous medium. The stresses in the porous solid and the fluid pressures in the pores can be given as:

$$\langle \tau_s \rangle_{ij} = (a_{11} u_{k,k} + a_{12} v_{k,k} + a_{13} w_{k,k}) \delta_{ij} + a_{10} (u_{i,j} + u_{j,i})$$
$$\langle \tau_g \rangle_{ij} = (a_{21} u_{k,k} + a_{22} v_{k,k} + a_{23} w_{k,k}) \delta_{ij}$$
$$\langle \tau_l \rangle_{ij} = (a_{31} u_{k,k} + a_{32} v_{k,k} + a_{33} w_{k,k}) \delta_{ij} \tag{3}$$

where δ_{ij} is the Kronecker symbol. a_{10} and $a_{ij}(i,j = x,y,z)$ are said to be elasticity constants with property $a_{ij} = a_{ji}$, and can be written as:

$$a_{10} = G_{fr}, \quad a_{11} = K_{fr} - \frac{2}{3} G_{fr}, \quad a_{12} = a_{21} = K_g S_g \alpha_s (K_l + \gamma)/K,$$
$$a_{13} = a_{31} = K_l \alpha_s (1 - S_g)(K_g + \gamma)/K, \quad a_{22} = K_g \alpha_g (K_l S_g + \gamma)/K,$$
$$a_{23} = a_{32} = K_g K_l S_g \alpha_l / K, \quad a_{33} = K_l \alpha_l [K_g (1 - S_g) + \gamma]/K$$
$$K = K_g (1 - S_g) + K_l S_g + \gamma, \quad \gamma = (1 - S_g) K_{cap}$$

where K_{cap} is called the macroscopic capillary pressure, Garg and Nayfeh (1986). K_{fr}, K_g and K_l are said to be the bulk modulus of the porous frame, gas phase and liquid phase, respectively. G_{fr} denotes the shear modulus for the porous solid. $S_i = \alpha_i/(1 - \alpha_s)(i = g, l)$ with $S_g + S_l = 1$ are the gas saturation and liquid saturation for the porous solid.

In terms of the displacement components, the equations of motion are expressed using Eq. (3) in Eq. (1):

$$(a_{10} + a_{11}) u_{j,ij} + a_{12} v_{j,ij} + a_{13} w_{j,ij} + a_{10} u_{i,jj} = \langle \rho_s \rangle \frac{\partial^2 u_i}{\partial t^2} - d_g \frac{\partial}{\partial t}(v_i - u_i) - d_l \frac{\partial}{\partial t}(w_i - u_i)$$
$$a_{21} u_{j,ij} + a_{22} v_{j,ij} + a_{23} w_{j,ij} = \langle \rho_g \rangle \frac{\partial^2 v_i}{\partial t^2} + d_g \frac{\partial}{\partial t}(v_i - u_i)$$
$$a_{31} u_{j,ij} + a_{32} v_{j,ij} + a_{33} w_{j,ij} = \langle \rho_l \rangle \frac{\partial^2 w_i}{\partial t^2} + d_l \frac{\partial}{\partial t}(w_i - u_i) \tag{4}$$

For solving Eq. (4) harmonically, we assume the displacements component as

$$(u_j, v_j, w_j) = (H_j, J_j, L_j)e^{i\omega(p_1x_1+p_2x_2+p_3x_3-t)} \tag{5}$$

where, ω is the angular frequency and $p_k(k=1,2,3)$ is the component of the slowness vector $\mathbf{p}$. The vectors $H = (H_{x_1}, H_{x_2}, H_{x_3})^T$, $J = \left(J_{x_1}, J_{x_2}, J_{x_3}\right)^T$ and $L = (L_{x_1}, L_{x_2}, L_{x_3})^T$ define the polarizations for the motions of solid, gas and liquid particles in porous medium. Substituting Eq. (5) in Eq. (4) then we get

$$\left[(a_{10}+a_{11})\mathbf{p}^T\mathbf{p} + \{a_{10}\mathbf{p}\mathbf{p}^T - b_{11}\}\right]\mathbf{H} + \left[a_{12}\mathbf{p}^T\mathbf{p} + b_{12}\right]\mathbf{J} + \left[a_{13}\mathbf{p}^T\mathbf{p} + b_{13}\right]\mathbf{L} = 0 \tag{6}$$

$$\left[a_{12}\mathbf{p}^T\mathbf{p} + b_{12}\right]\mathbf{H} + \left[a_{22}\mathbf{p}^T\mathbf{p} - b_{22}\right]\mathbf{J} + a_{23}\mathbf{p}^T\mathbf{p}\mathbf{L} = 0 \tag{7}$$

$$\left[a_{13}\mathbf{p}^T\mathbf{p} + b_{13}\right]\mathbf{H} + a_{23}\mathbf{p}^T\mathbf{p}\mathbf{J} + \left[a_{33}\mathbf{p}^T\mathbf{p} - b_{33}\right]\mathbf{L} = 0 \tag{8}$$

$\{b_{ij}\}$ are given by

$$b_{11} = \langle\rho_s\rangle + \frac{i}{\omega}(d_1+d_2), \quad b_{12} = \frac{i}{\omega}d_1, \quad b_{13} = \frac{i}{\omega}d_2,$$
$$b_{22} = \langle\rho_g\rangle + \frac{i}{\omega}d_1, \quad b_{33} = \langle\rho_l\rangle + \frac{i}{\omega}d_2$$

where, $\mathbf{I}$ is the identity matrix of order three and $\mathbf{p}^T$ denotes the conjugate transpose of the slowness vector $\mathbf{p}$. For simplification of Eqs. (6)–(8), we relate the polarization vectors of fluids in the form of the polarization vector of the solid with the help of Eqs. (7) and (8) as

$$\mathbf{J} = \mathbf{A}\mathbf{H}, \quad \mathbf{A} = -\frac{A_3}{A_6}\mathbf{I} + \frac{AA_1\lambda + AA_0}{A_4\lambda^2 + A_5\lambda + A_6}\mathbf{p}^T\mathbf{p}, \quad \lambda = \mathbf{p}\mathbf{p}^T \tag{9}$$

$$\mathbf{L} = \mathbf{B}\mathbf{H}, \quad \mathbf{B} = \frac{B_3}{A_6}\mathbf{I} - \frac{BB_1\lambda + BB_0}{A_4\lambda^2 + A_5\lambda + A_6}\mathbf{p}^T\mathbf{p} \tag{10}$$

Eqs. (9) and (10) show the displacement relations for liquid and gas particles with solid particles. On applying Eqs. (9) and (10) in Eq. (6), we find a system of three equations, which are

$$\Gamma\mathbf{H} = 0, \quad \Gamma = \gamma_1\mathbf{p}^T\mathbf{p} + \gamma_2(\lambda\mathbf{I} - \mathbf{p}^T\mathbf{p}) \tag{11}$$

Eq. (11) describes propagation phenomena in the medium and these equations are said to be Christoffel equations for elastic wave propagation in porous media. The coefficients used in the various relations, are

$$\gamma_1 = (a_{10}+f_{10})\lambda + \frac{\eta_1\lambda^2 + \eta_2\lambda + \eta_3}{A_4\lambda^2 + A_5\lambda + A_6}\lambda - f_{11}, \quad \gamma_2 = (a_{10}\lambda - f_{11}),$$
$$\eta_1 = a_{12}AA_1 - a_{13}BB_1, \quad \eta_2 = a_{12}AA_0 + b_{12}AA_1 - a_{13}BB_0 - b_{13}BB_1,$$
$$\eta_3 = b_{12}AA_0 - b_{13}BB_0, \quad f_{10} = a_{11} + \frac{B_3a_{13} - A_3a_{12}}{A_6},$$
$$f_{11} = b_{11} + \frac{A_3b_{12} - B_3b_{13}}{A_6},$$
$$AA_0 = \frac{A_3A_5 - A_2A_6}{A_6}, \quad AA_1 = \frac{A_3A_4 - A_1A_6}{A_6}, \quad BB_0 = \frac{B_3A_5 - B_2A_6}{A_6},$$
$$BB_1 = \frac{B_3A_4 - B_1A_6}{A_6}, \quad A_1 = a_{12}a_{33} - a_{13}a_{23},$$
$$A_2 = b_{12}a_{33} - b_{33}a_{12} - b_{13}a_{23},$$
$$A_3 = -b_{12}b_{33}, \quad A_4 = a_{22}a_{33} - a_{23}^2, \quad A_5 = -b_{22}a_{33} - b_{33}a_{22},$$
$$A_6 = b_{22}b_{33}, \quad B_1 = a_{12}a_{23} - a_{13}a_{22},$$
$$B_2 = b_{12}a_{23} - b_{13}a_{22} + a_{13}b_{22}, \quad B_3 = b_{13}b_{22},$$

The slowness vector is defined in terms of velocity V as $\mathbf{p} = \frac{\mathbf{N}}{V}$ such that $\mathbf{N}\mathbf{N}^T = 1$ and $\lambda = \frac{1}{V^2}$. The complex vector $\mathbf{N}$ represents the directions of propagation and attenuation of a wave in the porous medium and $\mathbf{N}^T$ is its conjugate transpose. In terms of $\mathbf{N}$ and V, the Christoffel Eq. (11) are expressed as

$$\left[\gamma_1\mathbf{N}^T\mathbf{N} + \gamma_2(\mathbf{I} - \mathbf{N}^T\mathbf{N})\right]\mathbf{H} = 0 \tag{12}$$

For non-trivial solutions for Eq. (12), the determinant $(= \gamma_1\gamma_2^2)$ must be zero. This provides us with two conditions

The first one (i.e. $\gamma_1 = 0$) gives

$$f_{11}A_6V^6 + \{f_{11}A_5 - \eta_3 - A_6(a_{10}+f_{10})\}V^4 + \{f_{11}A_4 - \eta_2 - A_5(a_{10}+f_{10})\}V^2 - \{\eta_1 + A_4(a_{10}+f_{10})\} = 0 \tag{13}$$

From the solution of Eq. (13), we get three complex velocities $(V_j, j=1,2,3)$ for the three attenuating waves that propagate in the porous medium. In the present case, for any of these three waves, the polarization vector $(H_{x_1}, H_{x_2}, H_{x_3})$ is found to be parallel to $\mathbf{N}$ and hence these three waves are identified as longitudinal body waves. These three waves with velocities $\Re(V_1), \Re(V_2)$, and $\Re(V_3)$ (where, $\Re(V_1) > \Re(V_2) > \Re(V_3)$) are identified as P_s, P_l, and P_g, respectively. The third wave is identified for the presence of the second fluid phase in pores.

The second one (i.e. $\gamma_2 = 0$) gives

$$f_{11}V^2 - a_{10} = 0 \tag{14}$$

From the solution of Eq. (14), we get a complex velocity $V_4 = \sqrt{\frac{a_{10}}{f_{11}}}$ for the single dispersive wave. The corresponding polarization vector $(H_{x_1}, H_{x_2}, H_{x_3})$ is parallel to any of the column (or, row) vectors of the singular matrix $(\mathbf{I} - \mathbf{N}^T\mathbf{N})$. This indicates the propagation of a single transverse (S) body wave in a porous medium with velocity V_4.

The polarizations of the gas and liquid particles can be calculated from Eqs. (9) and (10) for a given polarization vector of solid particles.

2.2. Cracked elastic solid

Wave anisotropy in the medium is caused by the presence of vertically aligned parallel cracks. The anisotropic parameters $(\varepsilon, \gamma, \delta)$ can be represented in terms of crack density (η) and crack porosity (φ_c) of the parallel cracks present in the elastic solid, Thomsen (1995). These relations can be given as:

$$\varepsilon = \frac{\frac{E}{\bar{E}} - 1}{2(1-\nu^2)}, \quad \gamma = \frac{1}{2}\left(\frac{\mu}{\bar{\mu}} - 1\right), \quad \delta = \frac{\Delta}{2(1-\nu)(1-\Delta)} \tag{15}$$

with

$$\Delta = \frac{\mu}{\bar{\mu}}\left(\frac{E}{\bar{E}} - 1\right)\frac{(1-\nu)}{(1+\nu)} + \left(\frac{\mu}{\bar{\mu}} - 1\right)(1-2\nu) \tag{16}$$

where the coefficients E and μ represent the Young's modulus and rigidity constant for the elastic solid in the absence of cracks. ν is the Poisson's ratio for the solid grains. Also, $\bar{E}$ and $\bar{\mu}$ represent the Yong's modulus and rigidity constant for presence of cracks in elastic medium. With the help of Eqs. (15) and (16), the effect of cracks on the elastic constants is defined as

$$\frac{E}{\bar{E}} = 1 + \eta\frac{16}{3}\left(1 - \frac{K_f}{K_s}\right)(1-\nu^2)D_c, \quad \frac{\mu}{\bar{\mu}} = 1 + \eta\frac{16}{3}\frac{(1-\nu)}{(2-\nu)} \tag{17}$$

where, $D_c = \left[1 - \frac{K_f}{K_s}\left(1 - \frac{16}{9}\frac{\eta}{\varphi_c}\frac{(1-\nu^2)}{(1-2\nu)}\right)\right]^{-1}$ is called the influence factor. K_s and K_f denote the bulk modulus of the solid and fluid, respectively. The crack porosity can be written as $\varphi_c = \frac{4}{3}\pi\eta\frac{c}{a}$. Where, η and $\left(\frac{c}{a}\right)$ represent the crack density and the aspect ratio of radius a and thickness c of the circular cracks. Anisotropic parameters are related to the elastic constants as

$$\varepsilon = \frac{1}{2}\left(\frac{C_{11}}{C_{33}} - 1\right), \quad \gamma = \frac{1}{2}\left(\frac{C_{66}}{C_{44}} - 1\right), \quad \delta = \frac{(C_{13}+C_{44})^2}{C_{33}(C_{33}-C_{44})} + \frac{C_{44}}{C_{33}} - 1 \tag{18}$$

Where $C_{11}, C_{13}, C_{33}, C_{44}$ and C_{66} are the elastic constants for the transversely isotropic elastic solid. Transverse isotropy can be reduced to the isotropy with the following relations: $C_{33} = C_{13} + 2C_{66}$ and $C_{44} = C_{66}$. The transversely isotropic behaviour of the cracked elastic solid can be represented by the values of elastic parameters $C_{33}, C_{44}, K_s, K_f, v, \eta$ and φ_c

2.3. Propagation and attenuation

From the previous section, we find four attenuated waves, propagating in an immiscible fluid saturated porous medium. Of these three are longitudinal body waves and the other is a transverse body wave. The propagation of an attenuated wave in a dissipative porous medium is defined through a complex slowness vector and its real and imaginary parts represent the propagation and the attenuation vector. The difference between the direction of propagation and the attenuation vector is said to be the inhomogeneity of a plane attenuated wave and this wave in a dissipative medium is known as an inhomogeneous wave, Borcherdt (1982).

For the representation of these waves, Sharma (2008b) has used a non dimensional parameter (δ) called the inhomogeneity parameter. The complex slowness vector $\mathbf{p}$ of an inhomogeneous wave in terms of (δ) can be written as:

$$\mathbf{p} = \frac{1}{v}\left[\hat{\mathbf{n}} + i\beta\hat{\mathbf{n}} + i\delta\widehat{\mathbf{m}}\right] \tag{19}$$

where, $\widehat{\mathbf{m}}$ is said to be the orthogonal unit vector of the propagation direction $\hat{\mathbf{n}}$. The vector $(\beta/v)\hat{\mathbf{n}}$ is said to be the attenuation along the propagation of the attenuated plane waves. Hence, the first two terms of Eq. (19) represent the propagation of a homogeneous wave and its homogeneous attenuation. The third term of Eq. (19) represents the propagation of an inhomogeneous wave. The total attenuation for an inhomogeneous wave is defined by the magnitudes $\sqrt{(\beta^2+\delta^2)}/v$. For $\delta = 0$, the attenuated wave is conceived to propagate as a homogeneous wave. For the propagation of the inhomogeneous attenuated wave $\delta \neq 0$. For our study, we need to determine the value of the attenuation coefficient β and the phase velocity v by using the given values of $\hat{\mathbf{n}}, \widehat{\mathbf{m}}$ and $\delta\epsilon\ [0,1)$.

Eq. (19) can be written as with the help of $\mathbf{p} = \frac{\mathbf{N}}{V}$ and $\mathbf{N}\mathbf{N}^T = 1$.

$$v^2 = -2\beta\frac{|h|^2}{\Im(h)}, \quad \beta = \frac{\Re(h)}{\Im(h)} + \sqrt{\left(\frac{\Re(h)}{\Im(h)}\right)^2 + 1 - \delta^2},$$
$$\mathbf{N} = \frac{(1+i\beta)\hat{\mathbf{n}} + i\delta\widehat{\mathbf{m}}}{\sqrt{1-\beta^2-\delta^2+2i\beta}} \tag{20}$$

where, $h = V^2$. The relation between the attenuation coefficient α and wave inhomogeneity (δ) can be given as

$$\alpha = \omega\sqrt{\beta^2+\delta^2}/v \tag{21}$$

3. Formulation of the problem

The aim of the present study is to understand the effect of vertical aligned cracks present in the elastic half space on the energy share of the incident wave by four reflected waves and two refracted waves at the loosely bonded interface between the cracked elastic half space and partially saturated porous half space. This study provides a mathematical model to analyze the continuous accumulation of the stress around the focal region of possible failure. The expansion of cracks is the most direct effect of accumulation of stress before an earthquake. On increasing the stress, the shape of the cracks change through changes in orientation, density and thickness of the solid. In the crust, changes in cracks may be responsible for an impending earthquake. We consider the possible changes in reflection or refraction coefficients for the incident wave as precursors, during the period of an earthquake. For the present study, we assume one of the medium is a partially saturated porous half space and the other one is a transversely isotropic cracked elastic half space. The transverse isotropy in the elastic medium is possible only on the presence of vertically aligned micro-cracks (Crampin, 1985). The change in crack shapes due to stress accumulation are shown here as changes in elastic anisotropy.

3.1. Definition of the problem

We consider a Cartesian coordinate system (x_1, x_2, x_3) to represent a 3-D space. Here, the interface between these two media can be represented by $x_3 = 0$, see Fig. 1. An attenuated wave with velocity V_0 travels through the medium-I (i.e. $x_3 > 0$) and is incident at a point on the interface making an angle θ_0 with the normal to the interface. For the study of propagation and attenuation of elastic waves, the problem has been considered for the x_1–x_3 plane. So, a unit vector $n = (\sin\theta, 0, -\cos\theta)$ represents the propagation direction of the incident wave and $m = (\cos\theta, 0, \sin\theta)$ represents its orthogonal direction. The geometry of the present problem clarifies that the incident angle (θ) varies from 0° to 90°. The slowness vector for an incident wave is given by $\mathbf{p} = (\sin\theta_0, 0, -\cos\theta_0)/V_0$, where V_0 is the complex velocity of the incident wave. The incident wave results in four reflected waves (P_p, P_l, P_g and SV) and two refracted waves (qP and qSV). According to Snell's law $\left(p_1 = \frac{\sin\theta_0}{V_0} = \frac{\sin\theta_1}{V_1} = \ldots\right)$, horizontal slowness will be same for incident, reflected and refracted waves. Therefore, the slowness vectors for reflected and refracted waves can be written as $(p_1, 0, q_k)$, (k = 1 to 6), where $q_k = \sqrt{1/V_k^2 - p_1^2}$.

The displacement for solid particles in a porous medium is given by

$$u_j = H_j^0 e^{i\omega(p_1x_1+q_0x_3-t)} + \sum_{k=1}^{4} f_k H_j^k e^{i\omega(p_1x_1+q_kx_3-t)}, \quad (j = x_1, x_3) \tag{22}$$

where, f_k is the excitation factor for reflected waves $(k = 1-4)$. Based on the propagation direction of the incident wave, we must have $\Re(q_0) < 0$. The corresponding displacement of gas and liquid particles can be calculated from Eq. (5) by using the matrices $\mathbf{J}$ and $\mathbf{L}$.

The particle motion in a cracked elastic solid (medium-II, i.e. $x_3 < 0$) is represented by the quasi-longitudinal (qP) wave and quasi transverse (qSV) wave. The displacement components $(U_{x_1}, 0, U_{x_3})$ in the cracked elastic solid half space are given as

$$U_{x_1} = \sum_{k=5}^{6} f_k e^{i\omega(p_1x_1+q_kx_3-t)}, \quad U_{x_3} = \sum_{k=5}^{6} R_k f_k e^{i\omega(p_1x_1+q_kx_3-t)} \tag{23}$$

where, f_k is the excitation factor for refracted waves $(k = 5, 6)$. The coupling constants R_k are given by Sharma (1999).

$$R_k = -\frac{(C_{11}p_1^2 + C_{44}q_k^2 - \rho)}{(C_{13}+C_{44})p_1q_k}, \quad (k = 5, 6) \tag{24}$$

The vertical slowness vector can be found from Sharma (1999)

$$C_{33}C_{44}q^4 + \left[\left(C_{11}C_{33} - C_{13}^2 - 2C_{13}C_{44}\right)p_1^2 - \rho(C_{33}+C_{44})\right]q^2 + C_{11}C_{44}p_1^4 - \rho(C_{11}+C_{44})p_1^2 + \rho^2 = 0 \tag{25}$$

From Eq. (25), we get two complex quantities for vertical slowness q^2. For numerical verification of the model, the values for q_5 and q_6 must satisfy the condition that is $\Re(q) < 0$. The stress components

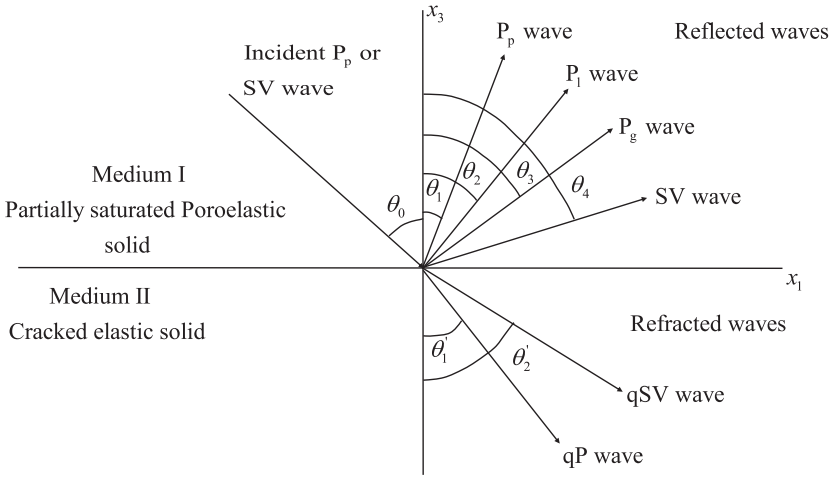

Fig. 1. Geometry of the problem.

on the x_1–x_3 plane with the normal along the x_3-direction are given by

$$\langle\sigma\rangle_{x_1x_3} = C_{44}\left(\frac{\partial U_{x_1}}{\partial x_3}+\frac{\partial U_{x_3}}{\partial x_1}\right), \quad \langle\sigma\rangle_{x_3x_3} = C_{13}\frac{\partial U_{x_1}}{\partial x_1}+C_{33}\frac{\partial U_{x_3}}{\partial x_3} \tag{26}$$

4. Boundary conditions

The boundary conditions at the interface between two layers are defined as the continuity of displacement components and stress components, Deresiewicz and Skalak (1963). Here, the restriction of fluid flow from the porous solid to the cracked elastic solid is considered. If at the interface, the surface of the pores is not fully sealed then the pore fluid can pass through the interface and come into contact with the elastic solid. This is possible only in the presence of the liquid in the porous skeleton. This type of condition is said to be loosely contacted between the porous solid and the elastic solid, Vashisth et al. (1991). For mathematical representation of the loose bonding, they proposed that the tangential stress at the interface is proportional to the tangential slip. So, the appropriate boundary conditions for loosely bonded interface at $x_3 = 0$ are.

(i) $\langle\tau_s\rangle_{x_3x_3} + \langle\tau_g\rangle_{x_3x_3} + \langle\tau_l\rangle_{x_3x_3} = \langle\sigma\rangle_{x_3x_3}$,
(ii) $\langle\tau_s\rangle_{x_3x_1} = \langle\sigma\rangle_{x_3x_1}$,
(iii) $\dot{v}_{x_3} - \dot{u}_{x_3} = 0$,
(iv) $\dot{w}_{x_3} - \dot{u}_{x_3} = 0$,
(v) $\alpha_s u_{x_3} + \alpha_1 v_{x_3} + \alpha_2 w_{x_3} = U_{x_3}$,
(vi) $\psi\langle\tau_s\rangle_{x_3x_1} = (1-\psi)Z\left(\dot{u}_{x_1} - \dot{U}_{x_1}\right)$

where, the parameter ψ is said to be the bonding constant and its range is $0 \leqslant \psi \leqslant 1$. $\psi = 1$ represents a smooth interface and $\psi = 0$ represents a welded interface at $x_3 = 0$. The finite constant Z is said to be the surface flow impedance for the fluid phase, Denneman et al. (2002). For the present study, we assume that the bonding constant has its value in between 0 and 1 ($0 < \psi < 1$). With the help of Eqs. (22) and (23), the above boundary conditions are satisfied by a system of six linear equations in f_1, f_2, f_3, f_4, f_5, and f_6. This system of equations can be written in combined form as

$$\sum_{k=1}^{4} L_{ik}f_k - \sum_{k=5}^{6} M_{ik}f_k = -L_{i0}, \quad (i = 1,2,\ldots,6) \tag{27}$$

where, the coefficients L_{ik}, (i = 1, 2, …, 6, k = 0, 1, …, 4) and M_{ik}, (i = 1, 2, …, 6, k = 5, 6) can be expressed as

$$\begin{aligned}
L_{1k} &= (X_{11}^{(k)} + Y_{11}^{(k)} + Z_{11}^{(k)})p_1S_1^{(k)} + (2a_{10} + X_{33}^{(k)} + Y_{33}^{(k)} + Z_{33}^{(k)})q_kS_3^{(k)} \\
&\quad + \left(D_1A_{31}^{(k)} + D_2B_{31}^{(k)}\right)\left(q_kS_1^{(k)} + p_1S_3^{(k)}\right), \\
L_{2k} &= a_{10}(S_1^{(k)}q_k + p_1S_3^{(k)}), \quad L_{3k} = (A_{31}^{(k)}S_1^{(k)} + (A_{33}^{(k)} - 1)S_3^{(k)}), \\
L_{4k} &= (B_{31}^{(k)}S_1^{(k)} + (B_{33}^{(k)} - 1)S_3^{(k)}), \\
L_{5k} &= \alpha_sS_3^{(k)} + \alpha_1(A_{31}^{(k)}S_1^{(k)} + A_{33}^{(k)}S_3^{(k)}) + \alpha_2(B_{31}^{(k)}S_1^{(k)} + B_{33}^{(k)}S_3^{(k)}), \\
L_{6k} &= \psi a_{10}(q_kS_1^{(k)} + p_1S_3^{(k)}) + (1-\psi)ZS_1^{(k)}, \quad (k = 0,1,2,3,4) \\
M_{1k} &= (C_{13}p_1 + C_{33}R_kq_k), \quad M_{2k} = C_{44}(q_k + R_kp_1), \\
M_{3k} &= M_{4k} = 0, \quad M_{5k} = R_k, \quad M_{6k} = (1-\psi)Z, \quad (k = 5,6)
\end{aligned}$$

where, $D_1 = a_{12} + a_{22} + a_{23}$, $D_2 = a_{13} + a_{23} + a_{33}$.

The matrices used in the previous equation can be defined as

$$\mathbf{X}^{(k)} = \left(a_{11} - \frac{2a_{10}}{3}\right)\mathbf{I} + a_{12}\mathbf{A}^{(k)} + a_{13}\mathbf{B}^{(k)},$$

$$\mathbf{Y}^{(k)} = a_{12}\mathbf{I} + a_{22}\mathbf{A}^{(k)} + a_{23}\mathbf{B}^{(k)}, \quad \mathbf{Z}^{(k)} = a_{13}\mathbf{I} + a_{23}\mathbf{A}^{(k)} + a_{33}\mathbf{B}^{(k)}$$

where, the matrices $\mathbf{A}^{(k)}$ and $\mathbf{B}^{(k)}$ are evaluated for each slowness vector $\mathbf{p}$ of the corresponding incident wave or reflected waves (k = 0, 1, …, 4).

To find the values of the excitation factor f_i, we solve Eq. (27) numerically with the help of the Gauss elimination method. The obtained values of $f_i (i = 1,2,\ldots,6)$ represent the amplitude ratios of the four reflected waves (P_p, P_l, P_g and SV) and the two refracted waves (qP and qSV) to the amplitude of the incident wave.

5. Energy ratios

In this section, we discuss the distribution of incident energy among the four reflected waves and the two refracted waves across a surface of unit area at the plane interface $x_3 = 0$. Following Achenbach (1973), the rate of energy transmission per unit surface area is given by the scalar product of the surface traction and the respective particle velocity represented by P^*. The average energy flux of the waves in the porous media, for a given surface with a normal along the x_3-direction is represented as

$$\langle P_{ij}^*\rangle = \Re\left[\langle\tau_s\rangle_{x_3x_1}^{(i)}\dot{u}_{x_1}^{(j)} + \langle\tau_s\rangle_{x_3x_3}^{(i)}\dot{u}_{x_3}^{(j)} + \langle\tau_1\rangle_{x_3x_3}^{(i)}\dot{v}_{x_3}^{(j)} + \langle\tau_2\rangle_{x_3x_3}^{(i)}\dot{w}_{x_3}^{(j)}\right], \quad (i,j = 0,1,\ldots,4) \tag{28}$$

The average energy flux of the refracted waves in the cracked elastic medium is defined as

$$\langle Q_{ij}^{*}\rangle = \Re\left[\langle\sigma\rangle_{x_3x_1}^{(i)}\dot{U}_{x_1}^{(j)} + \langle\sigma\rangle_{x_3x_3}^{(i)}\dot{U}_{x_3}^{(j)}\right], \quad (i,j=5,6) \tag{29}$$

The expression in the form of the matrix for the distribution of the incident energy among the four reflected waves is given by

$$E_{ij} = -\frac{\Re(F_{ij}f_i\bar{f}_j)}{\Re(F_{00})}, \quad (i,j=0,1,2,3,4) \tag{30}$$

and the two refracted waves

$$E_{ij} = -\frac{\Re(G_{ij}f_i\bar{f}_j)}{\Re(F_{00})}, \quad (i,j=5,6) \tag{31}$$

Here, the bar over a variable represents its complex conjugate. The matrix **F** and **G** can be given as

$$\begin{aligned}
F_{ij} = {} & \left[\left(Y_{11}^{(i)}\bar{A}_{31}^{(j)} + Z_{11}^{(i)}\bar{B}_{31}^{(j)}\right)p_1 + \left\{a_{10} + \left(a_{22}A_{31}^{(i)} + a_{23}B_{31}^{(i)}\right)\bar{A}_{31}^{(j)}\right.\right. \\
& \left.\left. + \left(a_{23}A_{31}^{(i)} + a_{33}B_{31}^{(i)}\right)\bar{B}_{31}^{(j)}\right\}q_i\right]S_1^{(i)}\bar{S}_1^{(j)} \\
& + \left[\left(Y_{33}^{(i)}\bar{A}_{31}^{(j)} + Z_{33}^{(i)}\bar{B}_{31}^{(j)}\right)q_i + \left\{a_{10} + \left(a_{22}A_{31}^{(i)} + a_{23}B_{31}^{(i)}\right)\bar{A}_{31}^{(j)}\right.\right. \\
& \left.\left. + \left(a_{23}A_{31}^{(i)} + a_{33}B_{31}^{(i)}\right)\bar{B}_{31}^{(j)}\right\}p_1\right]S_3^{(i)}\bar{S}_1^{(j)} + \left[\left(X_{11}^{(i)} + Y_{11}^{(i)}\bar{A}_{33}^{(j)} + Z_{11}^{(i)}\bar{B}_{33}^{(j)}\right)p_1\right. \\
& + \left\{\left(a_{12}A_{31}^{(i)} + a_{13}B_{31}^{(i)}\right) + \left(a_{22}A_{31}^{(i)} + a_{23}B_{31}^{(i)}\right)\bar{A}_{33}^{(j)}\right. \\
& \left.\left. + \left(a_{23}A_{31}^{(i)} + a_{33}B_{31}^{(i)}\right)\bar{B}_{33}^{(j)}\right\}q_i\right]S_1^{(i)}\bar{S}_3^{(j)}\left[\left(2a_{10} + X_{33}^{(i)} + Y_{33}^{(i)}\bar{A}_{33}^{(j)} + Z_{33}^{(i)}\bar{B}_{33}^{(j)}\right)q_i\right. \\
& + \left\{\left(a_{12}A_{31}^{(i)} + a_{13}B_{31}^{(i)}\right) + \left(a_{22}A_{31}^{(i)} + a_{23}B_{31}^{(i)}\right)\bar{A}_{33}^{(j)}\right. \\
& \left.\left. + \left(a_{23}A_{31}^{(i)} + a_{33}B_{31}^{(i)}\right)\bar{B}_{33}^{(j)}\right\}p_1\right]S_3^{(i)}\bar{S}_3^{(j)}
\end{aligned}$$

$$G_{ij} = (q_iC_{44} + C_{44}R_ip_1) + (C_{13}p_1 + C_{33}R_iq_i)R_j$$

The energy matrix E_{ij} defines the energy partition of the incident wave at the interface $x_3 = 0$. Further, the diagonal entries $E_{11}, E_{22}, E_{33}, E_{44}, E_{55}$ and E_{66} denote the energy shares of the four reflected P_p, P_l, P_g and SV waves and the two refracted qP and qSV waves. Due to the presence of the loose bonding between the given two media, tangential slip is allowed at the interface and this slip absorbs some of the incident energy. Because of loose bonding at the interface, the sum of the energy shares by reflected and refracted waves falls short that of the incident wave and this remaining energy share is said to be dissipated energy. The conservation of the total energy of the incident wave at the interface can be given by $E_{11} + E_{22} + E_{33} + E_{44} + E_{55} + E_{66} + E_{dissipated} = 1$.

6. Numerical results and discussion

For numerical verification of the proposed model, we have considered medium-I as a water and CO_2 saturated sandstone, in loose contact with basaltic rock (medium-II) containing uniformly distributed vertical aligned circular cracks. The material constants for each medium can be given as.

- **Medium-I: water and CO_2 saturated sandstone**: The material constants has been taken from Garg and Nayfeh (1986), are porosity $\varphi = 0.2$, $K_{fr} = 12$ GPa, $G_{fr} = 9$ GPa $\alpha_s = 0.8$, $\langle\rho_s\rangle = 2120\ \mathrm{kg\,m^{-3}}$, $K_g = 3.7$ MPa, $\langle\rho_g\rangle = 103S_g(1-\alpha_s)\ \mathrm{kg\,m^{-3}}$, $K_l = 2.7$ GPa, $\langle\rho_l\rangle = 990(1-S_g)(1-\alpha_s)\ \mathrm{kg\,m^{-3}}$, $K_{cap} = 0.1$ MPa. The values of dissipation coefficients are taken from Sharma and Saini (2012), $d_g = 0.04\ \mathrm{MPa{\cdot}s{\cdot}m^{-2}}$ and $d_l = 1\ \mathrm{MPa{\cdot}s{\cdot}m^{-2}}$.
- **Medium-II: basaltic rock with vertical aligned cracks**: the elastic constants C_{33} and C_{44} are given by $C_{33} = v_1^2\rho$ and $C_{44} = v_2^2\rho$. Where, v_1 and v_2 are the velocities of P and S waves and ρ is the density of the elastic medium. The values of velocities and densities are taken from Nandan and Saini (2012), are $v_1 = 5$ km/s, $v_2 = 2.75$ km/s, and $\rho_c = 2700\ \mathrm{kg/m^3}$. The other parameters are: $\frac{K_f}{K_s} = 0.053$, $\nu = 0.28$ and $Z = 1$ MPa·s/m.

The above numerical values have been used for the study of the distribution of energy share of the incident wave into the four reflected waves and two refracted waves from the loosely connected interface $x_3 = 0$. For the numerical analysis of the proposed model, we consider that the P_p and SV waves are incident on the interface $x_3 = 0$. The incident waves depend on the angle of the incidence (θ) which varies from 0° to 90°. The frequency for the present study of the energy shares of the incident wave is 1000 Hz. The variation of the energy ratios ($E_{11}, E_{22}, E_{33}, E_{44}, E_1, E_2$ and $E_{dissipated}$) with angle of incidence (θ) for presence and absence of vertically aligned cracks with respect to different values of aspect ratio (c/a), crack density (η) and bonding constant (ψ) are shown in Figs. 2–4 (for the incident P_p wave) and in Figs. 5–7 (for the incident SV wave).

For given incident P_p wave, Fig. 2 shows the variation in energy ratios with respect to angle of incident (θ) wave for different values of the bonding constant (ψ). We have given a comparative study for presence $(\eta \neq 0)$ and absence $(\eta = 10^{-15} \approx 0)$ of cracks and found that in the study of wave propagation of elastic waves for the imperfectly connected interface has significant effect of the presence of cracks. Based on the values of bonding constant (ψ), we get a significant effect of ψ on the energy ratios. On changing the interface property from welded $(\psi = 0)$ to smooth $(\psi = 1)$, we note that in the presence of cracks, the reflected (P_l and P_g) waves and the refracted (qSV) wave propagate slowly in their respective media but reflected SV wave and refracted qP wave become stronger. At normal incidence, the dissipative energy become stronger in comparison to the other energy shares that shows the larger slip at loosely bonded interface.

As per the requirement of the present problem, the effect of aspect ratio (c/a) for circular cracks with fixed radius (a) but changeable crack thickness (c) on the energy ratios has been presented in Fig. 3. It is clear from Fig. 3 that on increase of the aspect ratio, the critical angle decreases in each figure of Fig. 3. All of the energy shares affect significantly close to the critical angle of the incidence. For postcritical incident of fast P_p wave, reflected P_g, P_l and SV waves reflect strongly with respect to the aspect ratio. At grazing incidence, most of the energy shares have been found in between reflected P_p and refracted qSV waves. Near the postcritical incidence, change in crack thickness has positive impact on the refracted qP wave but negative impact has been found on refracted qSV waves. Dissipated energy has negligible impact of the aspect ratio (c/a).

Fig. 4 presents the change in energy share of the incident waves by reflected and refracted waves at the loosely bonded interface $x_3 = 0$ for three different values of the crack density η. In which, we have given comparison between the presence $(\eta \neq 0)$ and absence $(\eta = 10^{-15} \approx 0)$ of cracks in basaltic rock. The critical angle for incident wave is found around 40° for each of the reflected and refracted waves except for the refracted qSV wave. It decreases with increase of crack density (η). Dissipated energy increases with respect to angle of incidence (θ) meaning more energy is absorbed at the loose interface with respect to the incident angle. After post critical incidence, we found that slow (P_l, P_g) and fast SV waves reflect strongly with increase of the crack density (η). For normal incidence of the P_p wave results there is no refracted qSV wave in the elastic medium. The effect of a change in crack density has been found to be very little on the fast reflected P_p wave, refracted qSV wave and on dissipated energy but for critical incidence, we see some strengthening in fast P_p wave. These results follow the conservation law of energy.

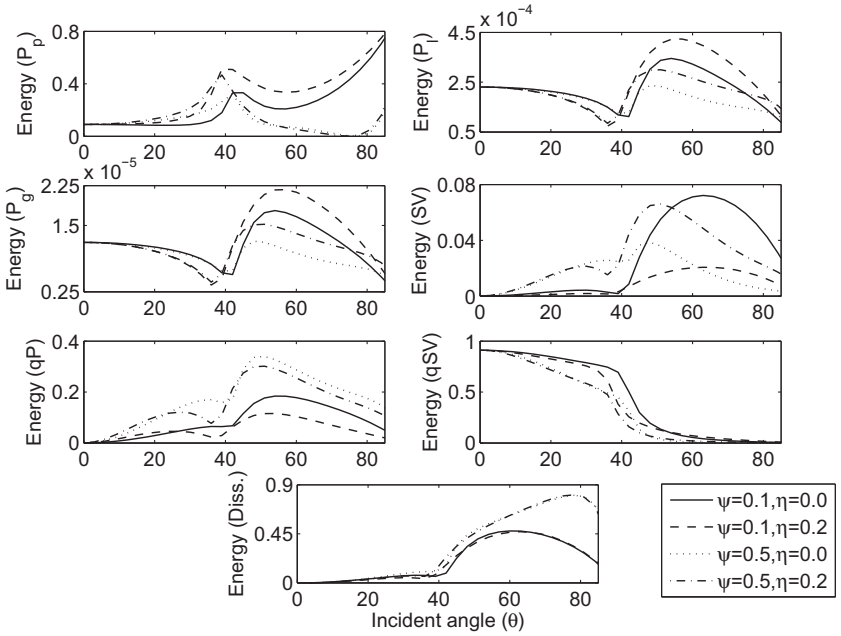

Fig. 2. Energy shares of incident P_p wave by the reflected (P_p, P_l, P_g, SV) waves, refracted (qP, qSV) waves and energy dissipation at the interface $x_3 = 0$ with incidence direction (θ) for different values of the bonding parameter (ψ) in the presence and absence of the vertically aligned cracks for given $S_g = 0.5, \delta = 0.02$ and $c/a = 0.01$.

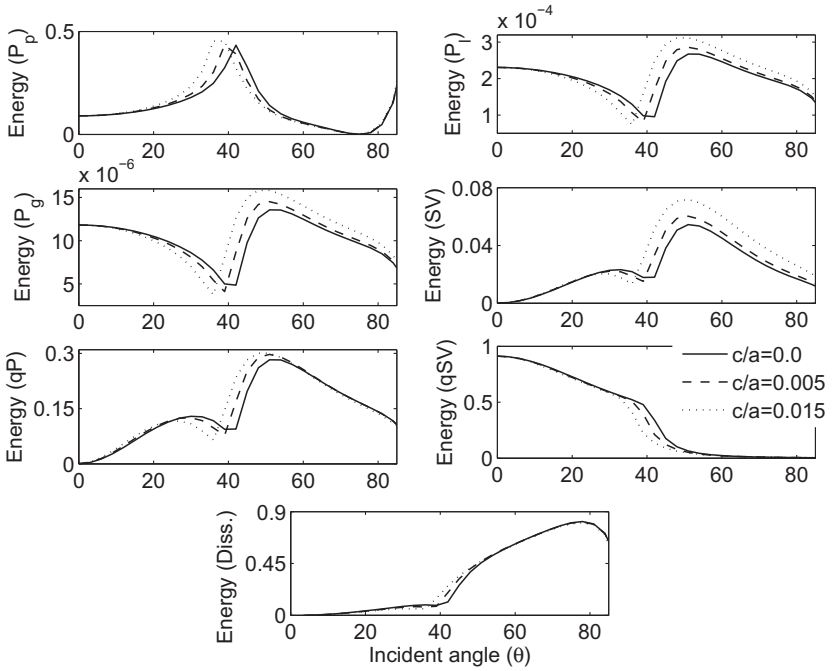

Fig. 3. Energy shares of incident P_p wave by the reflected (P_p, P_l, P_g, SV) waves, refracted (qP, qSV) waves and energy dissipation at the interface $x_3 = 0$ with incidence direction (θ) for different values of the aspect ratio (c/a) for given $S_g = 0.5,\ \delta = 0.02,\ \psi = 0.5$ and $\eta = 0.2$.

The change in energy shares with incident angle (θ) for different values of the bonding parameter ψ with respect to presence and absence of cracks in basaltic rocks is shown in Fig. 5. Significant effect of loose bonding has been found on all of the reflected waves, refracted waves and on dissipated energy. For the fixed value of bonding parameter, we find that the reflected P_p, P_l, P_g and refracted qP, qSV waves gain some strength in the absence of cracks but we find weaker dissipated energy. At grazing incidence, most of the energy share has been found among the refracted qP wave and the dissipated energy and for normal incidence, it is in the reflected SV wave. For the presence of aligned cracks in the elastic medium, we see a sudden change in energy share of the refracted qSV wave for a given incident angle in the range $42^\circ < \theta < 48^\circ$. This change shows that the refracted qSV wave will move towards the loosely bonded interface because of the negative sign of energy share. In the absence of cracks, we get weaker dissipated energy.

The effect of aspect ratio (c/a) on energy share at a loosely bonded interface is shown in Fig. 6. Very little impact of crack thickness (c) has been found on the refracted waves. Near the critical angle (around 48°), we get negative energy share of the refracted qSV wave that may give strength to the dissipative

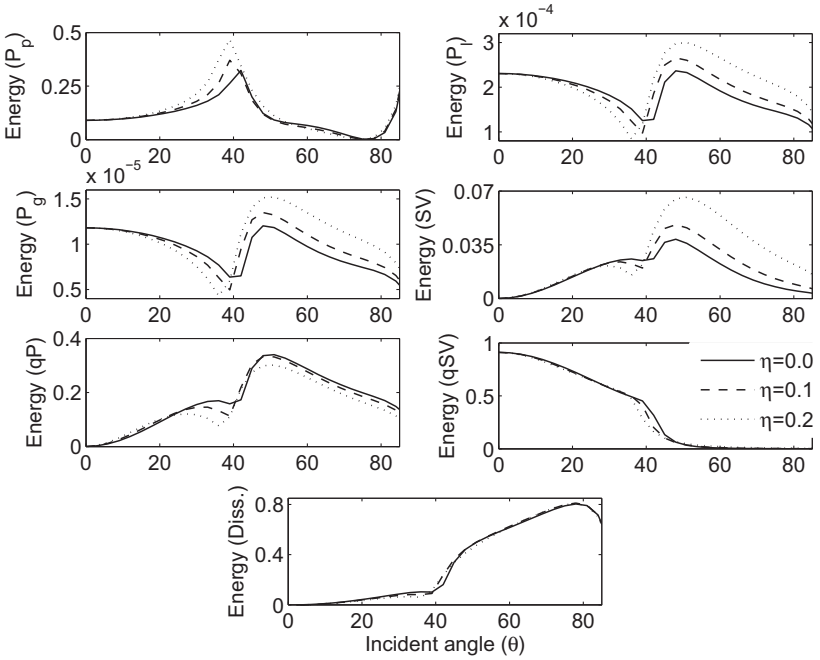

Fig. 4. Energy shares of incident P_p wave by the reflected (P_p, P_l, P_g, SV) waves, refracted (qP, qSV) waves and energy dissipation at the interface $x_3 = 0$ with incidence direction (θ) for different values of the crack density (η) for given $S_g = 0.5,\ \delta = 0.02,\ \psi = 0.5$ and $c/a = 0.01$.

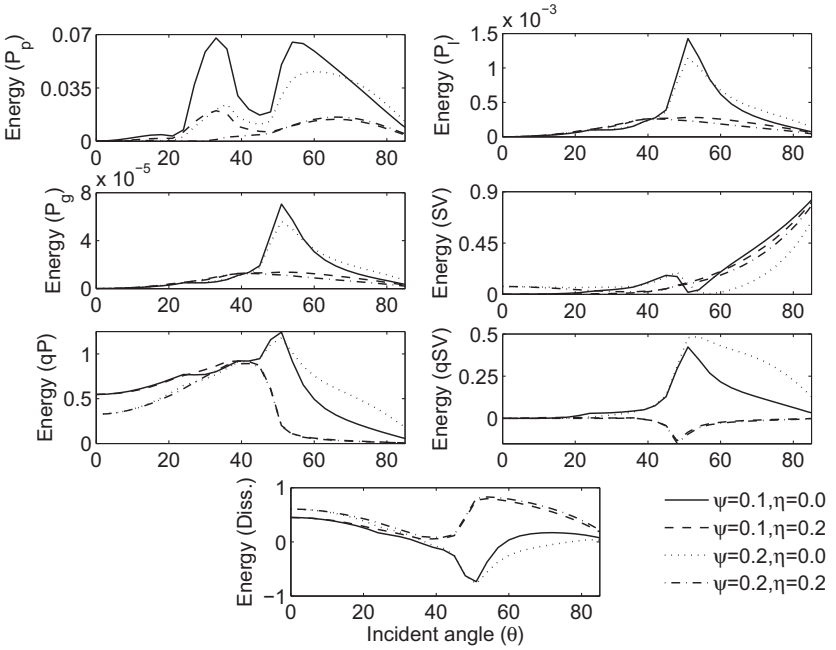

Fig. 5. Energy shares of incident SV wave by the reflected (P_p, P_l, P_g, SV) waves, refracted (qP, qSV) waves and energy dissipation at the interface $x_3 = 0$ with incidence direction (θ) for different values of the bonding parameter (ψ) in the presence and absence of the vertically aligned cracks for given $S_g = 0.5,\ \delta = 0.02$ and $c/a = 0.01$.

energy. The change in crack thickness has positive impact on the reflected P_p, P_l and P_g waves but has negative impact on reflected SV wave. At grazing incidence, most of the energy share of the incident SV wave has been distributed in between reflected SV wave and dissipated energy. At the grazing and normal incidence, no sign of refracted qSV wave is indicated through Fig. 6.

For the incidence of the SV wave, the effect of crack density η on the energy share is shown in Fig. 7. In the absence $\eta = 10^{-15} \approx 0$ of aligned cracks, we find that most of the incident energy distributes in between reflected and refracted waves and very less energy is dissipated at the interface. The critical angle for each wave except the fast P_p wave is found around 45° in presence $\eta \neq 0$ of aligned cracks but in the absence of aligned cracks, the critical angle is found around 50°. We get stronger reflected and refracted waves in absence of cracks in the elastic medium except for the reflected SV wave. The effect of the crack density has been found in refracted qP and qSV waves for the post critical incident angle. A sudden drop in energy share has been shown for the refracted qSV wave around the critical angle for the presence of aligned cracks. After postcritical incidence with reduction in the values of crack density, we see

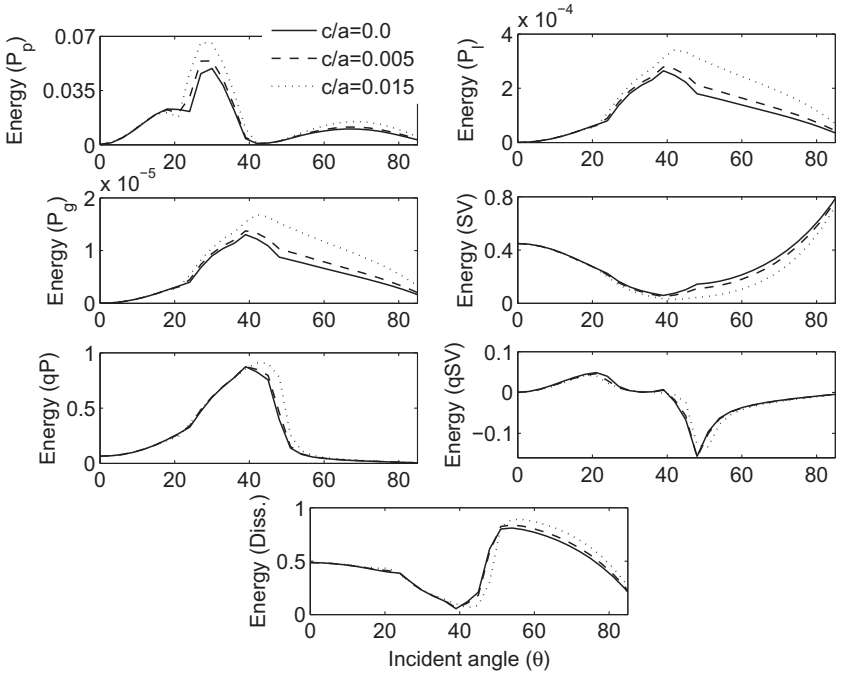

Fig. 6. Energy shares of incident *SV* wave by the reflected (P_p, P_l, P_g, SV) waves, refracted (qP, qSV) waves and energy dissipation at the interface $x_3 = 0$ with incidence direction (θ) for different values of the aspect ratio (c/a) for given $S_g = 0.5,\ \delta = 0.02,\ \psi = 0.5$ and $\eta = 0.2$.

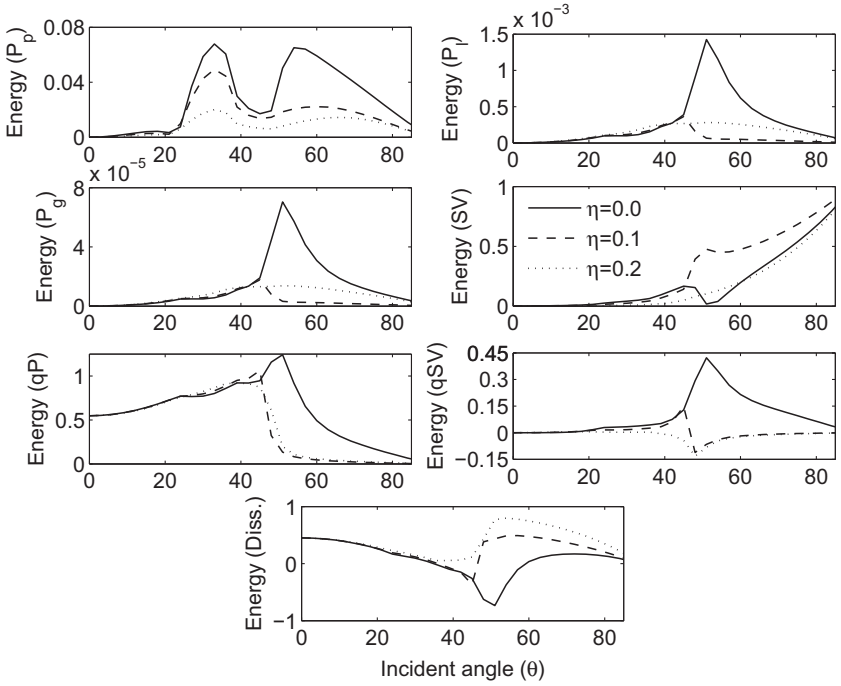

Fig. 7. Energy shares of incident *SV* wave by the reflected (P_p, P_l, P_g, SV) waves, refracted (qP, qSV) waves and energy dissipation at the interface $x_3 = 0$ with incidence direction (θ) for different values of the crack density (η) for given $S_g = 0.5,\ \delta = 0.02,\ \psi = 0.1$ and $c/a = 0.01$.

stronger reflected P_p, P_l and P_g waves and refracted qP and qSV waves but weaker dissipated energy. At grazing incidence, energy shares of reflected P_p, P_l and P_g waves are almost zero.

7. Conclusion

The effect of aspect ratio, crack density, and loose bonding parameteron inhomogeneous wave propagation along the interface between porous solid saturated by two immiscible fluids and cracked elastic half space has been studied. We have also given a comparative study with and without aligned cracks in the elastic half space. It is assumed that the vertical aligned cracks present in the elastic half space can be represented by the crack density and aspect ratio. It is also believed that both the media are loosely connected to each other assuming the tangential slip present at the interface, Vashisth et al. (1991). This slip absorbs part of the incident wave energy that results in weakening the reflected and refracted waves and is evident as dissipated energy. An analysis

of the effect of aspect ratio, crack density and bonding parameter on energy share is confirmed by a numerical example and we draw the following conclusions:

1. For a given incident P_p or SV wave, the vertically aligned cracks in the elastic half space give significant difference in the energy share of the incident wave by reflected and refracted waves. In the absence of the cracks for given incident SV wave, less energy will be absorbed at the loosely bonded interface in the form of dissipated energy.
2. We see significant change in the energy ratios with respect to changes in the bonding constant from welded to smooth interface that shows the importance of the type of interface between two media in wave propagation analysis. Our results successfully fulfill the claim that in the presence of loose boundary, the sum of energy shares of all scattered waves at the interface is short of unity. Overall it is clear that the assumption of loosely bonded interface for the present study in place of welded $(\psi = 0)$ or smooth $(\psi = 1)$ interface affects significantly the reflection–refraction phenomena. In the presence and absence of cracks, considerable change has been found for given values of bonding parameter.
3. In the presence of cracks for a given incident SV wave, a sudden energy drop has been found in case of refracted qSV wave for the given incident angle in the range of $42^\circ < \theta < 48^\circ$. It shows that the refracted qSV wave moves towards the loosely bonded interface because of the negative value of the energy share.
4. Change in crack density η or thickness (c) of the cracks (for the fixed radius) can directly affect the porosity $(\varphi_c = \frac{4}{3}\pi\eta\frac{c}{a})$ of the cracked elastic half space. In the presence of cracks, the change in crack thickness and crack density do not affect the refracted qP and qSV waves much but some changes have been found around the critical incidence for a given incident SV wave.
5. The energy shares of the reflected slow P_l and P_g waves of the incident wave are very small in comparison to the other energy shares.
6. We found that at grazing incidence of the SV wave, most of the incident energy is dissipated at the interface but in the case of the incident P_p wave very little or all most zero energy is dissipated around the interface.
7. Our results satisfy the conservation of the energy at the loosely bonded interface between the porous half space and the cracked elastic half space.

The effect of the presence of vertical aligned cracks in the elastic half space and tangential slip at loosely bonded interface on the energy share of the incident wave by the reflected and refracted waves may help to understand the reflection and refraction phenomena that are used in exploration seismology. Also, this study can be helpful for understanding the wave pattern of elastic waves from the loosely bonded interface. These cracks are mainly dependent on the crack density and thickness of the cracks and may directly be the cause of the accumulation of stresses before an earthquake. Such behaviour of these cracks in a particular region may be the indication of a precursor to an earthquake.

We know that most part of the earth's crust is basically rock, which may possibly be a heterogeneous, porous and cracked elastic solid. These rocks can contain oil, gas, water or some other minerals. This study may help us in obtaining information of the characteristics of fluid flow through sedimentary rock in the crust by using the process of the wave propagation in a realistic mathematical model that can be beneficial in petrolatum industries, seismic exploration, reservoir monitoring and geophysical studies of the earth's crust.

Acknowledgments

The authors convey their sincere thanks to Council of Scientific and industrial research (CSIR), New Delhi, for providing a SRF to Mr. Sushant Shekhar and also thank the Head CSIR-4PI, Bangalore for providing all facilities needed in this research work.

References

Achenbach, J.D., 1973. Wave Propagation in Elastic Solids. North-Holland, Amsterdam.
Ainslie, M.A., Burns, P.W., 1995. Energy-conserving reflection and transmission coefficients for a solid-solid boundary. J. Acoust. Soc. Am. 98, 2836–2840.
Bedford, A., Drumheller, D.S., 1983. Theories of immiscible and structured mixtures. Int. J. Eng. Sci. 21, 863–960.
Berryman, J.G., 2007. Seismic waves in rocks with fluids and fractures. Geophys. J. Int. 171, 954–974.
Biot, M.A., 1956a. General solutions of the equations of elasticity and consolidation for a porous material. J. Appl. Mech. 23, 91–95.
Biot, M.A., 1956b. Theory of propagation of elastic waves in a fluid-saturated porous solid, I. Low-frequency range. J. Acoust. Soc. Am. 28, 168–191.
Biot, M.A., 1962a. Mechanics of deformation and acoustic propagation in porous media. J. Appl. Phys. 33, 1482–1498.
Biot, M.A., 1962b. Generalized theory of acoustic propagation in porous dissipative media. J. Acoust. Soc. Am. 34, 1254–1264.
Biot, M.A., Willis, D.G., 1957. The elastic coefficients of the theory of consolidation. J. Appl. Mech. 24, 594–601.
Borcherdt, R.D., 1982. Reflection–refraction of general P and type-I S waves in elastic and anelastic solids. Geophys. J.R. Astron. Soc. 70, 621–638.
Brutsaert, W., 1964. The propagation of elastic waves in unconsolidated unsaturated granular medium. J. Geophys. Res. 69, 243–257.
Chatterjee, A.K., Knopoff, M., Hudson, J.A., 1980. Attenuation of elastic waves in a cracked, fluid saturated solid. Math. Proc. Cambridge Philos. Soc. 88, 547–561.
Crampin, S., 1978. Seismic wave propagation through a cracked solid: polarization as a possible dilatancy diagnostic. Geophys. J.R. Astron. Philos. Soc. 53, 467–496.
Crampin, S., 1985. Evidence for aligned cracks in Earth's crust. First Break 3, 12–15.
Crampin, S., 1987. The basis for earthquake prediction. Geophys. J.R. Astron. Soc. 91, 331–347.
Denneman, A.I.M., Drijkoningen, G.G., Smeulders, D.M.J., Wapenar, K., 2002. Reflection and transmission of waves at a fluid/porous medium interface. Geophysics 67, 282–291.
Deresiewicz, H., 1962. The effect of boundaries on wave propagation in liquid filled porous solid: IV. Surface waves in a half space. Bull. Seism. Soc. Am. 52, 793–799.
Deresiewicz, H., Skalak, R., 1963. On Uniqueness in dynamic poroelasticity. Bull. Seism. Soc. Am 53, 793–799.
Garg, S.K., Nayfeh, A.H., 1986. Compressional wave propagation in liquid and/or gas saturated elastic porous media. J. Appl. Phys. 60, 3045–3055.
Nandan, J.S., Saini, T.N., 2012. Reflection and refraction at an imperfectly bonded interface between poroelastic solid and cracked elastic solid. J. Seismolog. 17, 239–253.
O'Connell, R.J., Budiansky, B., 1974. Seismic velocities in dry and saturated cracked solids. J. Geophys. Res. 79, 5412–5426.
Sharma, M.D., 1999. Dispersion in oceanic crust during earthquake preparation. Int. J. Solids Struct. 36, 3469–3482.
Sharma, M.D., 2008a. Wave propagation across the boundary between two dissimilar poroelastic solids. J. Sound Vib. 314, 657–671.
Sharma, M.D., 2008b. Propagation of inhomogeneous plane waves in viscoelastic anisotropic media. Acta Mech. 200, 145–154.
Sharma, M.D., 2009. Boundary conditions for porous solids saturated with viscous fluid. Appl. Math. Mech. 30, 821–832.
Sharma, M.D., Gogna, M.L., 1991. Wave propagation in an anisotropic poroelastic liquid saturated porous solid. J. Acoust. Soc. Am. 89, 1068–1073.
Sharma, M.D., Saini, R., 2012. Wave propagation in porous solid containing liquid filled bound pores and two-phase fluid in connected pores. Eur. J. Mech. & Solids 36, 53–65.
Thomsen, L., 1995. Elastic anisotropy due to aligned cracks in porous rocks. Geophys. Prospect. 43, 805–829.
Tomar, S.K., Arora, A., 2006. Reflection and transmission of elastic waves ar an elastic/porous solid saturated by two immiscible fluids. Int. J. Solids Struct. 43, 1991–2013.
Tuncay, K., Corapcioglu, M.Y., 1997. Wave propagation in poroelastic media saturated by two fluids. J. Appl. Mech. 64, 313–320.
Vashisth, A.K., Sharma, M.D., Gogna, M.L., 1991. Reflection and transmission at a loosely bonded interface between liquid-saturated porous solid and elastic solid. Geophys. J. Int. 89, 1068–1073.
Xu, S., King, M.S., 1990. Attenuation of elastic waves in a cracked solid. Geophys. J. Int. 101, 169–180.
Yew, C.H., Jogi, P.N., 1976. Study of wave motions in a fluid-saturated porous rocks. J. Acoust. Soc. Am. 60, 2–8.